Nanoscale

PAPER

Check for updates

Cite this: *Nanoscale*, 2021, **13**, 2703

Analysis of dendrimer-protein interactions and their implications on potential applications of dendrimers in nanomedicine

James Magnus Rae[a] and Barbara Jachimska *[b]

Received 23rd October 2020,
Accepted 20th January 2021

DOI: 10.1039/d0nr07607d

rsc.li/nanoscale

This work addresses how G5.5 PAMAM dendrimers form complexes with bovine serum albumin (BSA). Analytical techniques, such as UV-vis spectrophotometry, dynamic light scattering, electrophoretic mobility, quartz crystal microbalance with dissipation monitoring (QCM-D), circular dichroism (CD), and contact angle were used to analyze the properties of the dendrimers systems. The binding of protein to dendrimers can alter the structure, mobility, conformation and functional activity of the dendrimer. The results show that BSA interactions with G5.5 dendrimer carriers are driven both by electrostatic and hydrophobic forces. Dendrimer surface charge is reduced upon contact with the protein. The protein shell formed on the surface of the carrier is very stable as evidenced by the QCM-D measurements. On the other hand, the CD spectra indicates a change in the secondary structure of the protein. The size of the changes is significantly dependent on the ratio of protein to dendrimer. Understanding the mechanism of interaction of potential carriers with proteins is important for their internalization into the cell.

Introduction

Despite the continuous advancement of nanotechnology and the development of many new drug delivery systems (DDS), nanomedicine still faces many challenges. M. Marques *et al.* in their review of Nanomedicine – Fine Particles and Big Challenges, presented several problems still waiting to be solved.[1] DDS are especially needed in cases of genetic disease where inhibition of development or protective effect is the only therapeutic method available today. Characterisation of nanotechnology related DDS requires a combination of various advanced analytical techniques to understand the physicochemical properties and their impact on performance and toxicity in the target environment.

Today, many types of biomaterials used in biomedicine require novel concepts for chemical manipulation and surface modification to create biological interfaces capable of mimicking the bioenvironment. Surface property requirements are different for each system, no one-size-fits-all model can be used to explain the interactions between biomaterial surfaces and body fluids. The challenge is, therefore, to create a biomaterial with appropriate volume and surface properties. However, it is impossible to modify the attributes of the surface by means of film deposition or coupling of active molecules for the optimal physical and chemical properties.

As a result of the growing demand for more complex and highly specific macromolecules research is now focused on highly branched dendrimer polymers. They have unique properties making them ideal candidates for nanoscale applications. The synthesis of dendrimers can be carefully controlled in terms of their size, shape, molecular weight, composition and reactivity. Dendrimers have hyperbranched structures with precisely located functional groups that allow the properties of the therapeutic molecules, which can be both encased inside the macromolecule and adhered to its outer surface, to be controlled. Of the numerous dendrimer compounds, poly(amidoamine) (PAMAM) dendrimers stand out because they were the first to be introduced to the market and belong to the most widely characterised dendrimer families. Dendrimers can be used as nanocarriers to increase the solubilisation of drugs and increase the effectiveness of drugs and improve therapeutic effects, or for targeted drug delivery through the use of ligands targeting specific cell receptors.

An essential issue in the application of dendrimer systems is the broadening of knowledge about their interactions with biological systems.[2] Nanoparticles entering biological systems are almost always covered with bioliquids. Therefore, in order to develop the selective delivery of nano-objects to individual body compartments, it is crucial to understand the phenomena related to conformational changes and protein displace-

[a]*Department of Chemical and Process Engineering, University of Strathclyde, 75 Montrose Street, Glasgow G1 1XJ, UK*
[b]*Jerzy Haber Institute of Catalysis and Surface Chemistry, Polish Academy of Sciences, Niezapominajek 8, PL-30239 Krakow, Poland.*
E-mail: barbarajachimska@ikifp.edu.pl

ment at the interface. From the nanomedical point of view, the phenomena of competitive binding and displacement of proteins, referred to as the Vroman effect,[3,4] are also extremely important, because they determine the selective delivery of nanoscale objects to specific body compartments.[5] Hydrophobic drug carriers are opsonised by proteins belonging to its complement proteins or antibodies, causing phagocytosis by macrophages or neutrophils. It is estimated that most of the opsonised particles are cleared from the bloodstream by the liver and spleen within five minutes after their administration.[6] Investigation of the binding kinetics of polymer nanoparticles with proteins in human plasma using a wide range of analytical techniques, including, for example, calorimetry, chromatography and surface plasmon resonance (SPR)[7,8] shows the formation of two types of protein coatings on the surface of nanoparticles: soft and hard corona. The size of the nanoparticles and the surface properties have a significant influence on the composition of the protein corona. The research shows that the coatings derived from the plasma on the surface of polystyrene nanoparticles and silica nanoparticles inhibit protein adsorption. The key unanswered questions are whether the observations and hypotheses for the interaction of proteins with relatively large and hard nanoparticles apply to small and softer organic nanostructures with sizes comparable to those of proteins.[9] from this point of view, dendrimers are ideal model systems for studying the interaction of soft organic nanomaterials with proteins found in biological fluids.

Materials and methods

Materials

Experiments were conducted on generation 5.5 poly(amidoamine) PAMAM dendrimers with ethylenediamine-based core and terminal carboxyl groups (Dendritech, Inc. Michigan; Midland, MI, USA). Bovine Serum Albumin (BSA;>99% protein, essentially fatty-acid free) was purchased from Sigma-Aldrich. Samples were prepared by dissolving in deionized water, adjusting the ionic strength using sodium chloride (NaCl) and the pH using hydro-chloric acid (HCl) or sodium hydroxide (NaOH) solutions. The pH of BSA and NaCl solutions was monitored using a precision WTW pH meter equipped with a Hamilton Polyplast Din electrode.

Methods

Dynamic light scattering (Malvern Nano ZS instrument) was used to determine the diffusion coefficient of the samples. The diffusion coefficient was then used to calculate the hydrodynamic diameter using Stokes equation.

Circular Dichroism (CD) was used to monitor the structure of G5.5/BSA complexes in a 0.01 M solution of NaCl at varied pH (in the range 3.0–10.0) using a Jasco-1500 spectrometer with a 10 nm quartz cuvette. Solvent base spectra were measured using 0.01 M NaCl under defined pH conditions. The spectra were recorded in the wavelength range 185–300 nm with a resolution of 1 nm and a scanning speed of 50 nm min^{-1}. Qualitative and quantitative analysis of the secondary structure of BSA under various pH conditions was carried out using Jasco software.

Quartz Crystal microbalance with energy dissipation (QCM-D) (QSense E1, Biolin Scientific) was used to determine the efficiency of dendrimer and BSA protein adsorption on the gold surface and the properties of the formed layer. The scattering monitoring module provides a description of the viscoelastic properties of the layer formed on the sensor. Sensors covered with a layer of gold were used for all measurements. Flow rates were controlled by a peristaltic pump (Ismatec). The adsorbed mass on the sensor for homogeneous, rigid films was calculated using the Sauerbrey model.

Contact angle was measured by determining sedentary water drop shape using axial symmetrical drop shape analysis (ADSA) with a system accuracy of 1°. A layer of G5.5 PAMAM and BSA was adsorbed on the gold sensor surface by the Q sense QCM-D equipment. The image of a drop of sitting water was obtained with a CCD video camera. The Young-Laplace equation was fitted to the digitized water drop profile on the sensor surface.

Results and discussion

Physicochemical properties of PAMAM dendrimer

Understanding the physicochemical properties of G5.5 PAMAM is essential for their applications. As shown by many studies, the transport of nanomaterials in cells depends on several critical physicochemical properties, such as size, shape, charge and hydrophobicity of the surface. These nanosystem parameters will determine its biodistribution.[10]

The hydrodynamic radius (R_H) this can be obtained from diffusion coefficient measurements using the dynamic light scattering technique (DLS). DLS measurements were carried out for samples of G5.5 PAMAM (c = 500 ppm) at three different ionic strengths; I = 0.0001 M, I = 0.01 M, and I = 0.15 M NaCl, using the Malvern Zetasizer. The values measured for the lowest ionic strength were noted to form aggregates at very low pH and at neutral pH. From the theory developed by Derjaguin, Verway, Landau and Overbeek on colloidal stability, it is understood that the ionic strength of the solution that suspends charged colloids exerts a degree of control over the electrostatic forces between particles.[11] With the stability determined by the Debye length and van der Waals forces of approaching particles. In this case we see that for higher ionic strength, there is a reduction in the favourable attractive interactions between the particles due to favourable screening effects from ions.[12] The experimental results of the DLS measurements are shown in Fig. 1.

From the results R_H was seen to increase with increasing pH. Values for R_H ranged from 3.35 nm to 4.35 nm. When pH was lower than 7.5 the mean R_H was found to be 3.50 nm and above pH 7.5 it was found to be 3.91 nm. The effect of changing the particle size is consistent with the direction of an increase in the degree of protonation of external functional

 This journal is © The Royal Society of Chemistry 2021

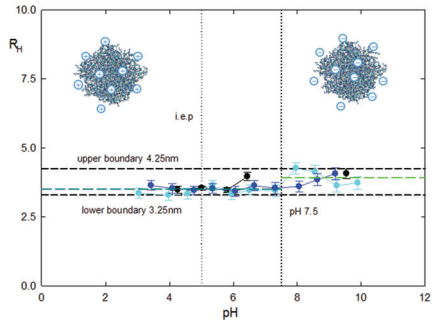


Fig. 1 Experimental results for hydrodynamic radius R_H at varied pH for G5.5 PAMAM c = 500 ppm. With the colour of points denoting variations in ionic strength. Black I = 0.001 M, blue I = 0.01 M and cyan I = 0.15 M.

groups. The steric interaction between groups in the outer layer increases the particle size. It also affects the degree of hydration of the entire system, the swelling effect of the dendrimer structure.

These values were then compared to other experimental data for G5.5 PAMAM size from literature where R_H was found to measure at 3.94 nm when calculated from the diffusion coefficient obtained from NMR measurements.[13,14]

In order to gain a good understanding of the process of complex formation, it is important to obtain the zeta potential measurements as this will provide information as to whether therapeutic agents or proteins will be complexed on the surface of the nanocarrier. It also aids the analysis of the adsorption process, a process in which the electrostatic interactions control the adsorption behaviour.[15,16] Electrophoretic mobility measurements were taken for G5.5 PAMAM (c = 1000 ppm) at varying ionic strengths (I = 0.0001 M, I = 0.01 M, I = 0.02 M, I = 0.05 M, I = 0.1 M and I = 0.15 M NaCl) across the pH range of 3–10. The electrophoretic mobility was then used to calculate the zeta potential using Henry's equation. The net charge of the dendrimer was found to be positive below pH 5, and negative above pH 5. The isoelectric point (IEP) was therefore found to be at pH 5 as shown in Fig. 2a. It can also be seen that the magnitude of the value for zeta potential measured at any given pH is lower for increased ionic strength. Samples with I = 0.01 M and lower were seen to have similar values, a jump was then observed for I = 0.02 M and then again to I = 0.05 M with values above this experiencing similar values.

The surface charge of the G5.5 PAMAM dendrimer is determined by its functional groups, it is built with 320 functional groups. There are 256 carboxyl surface groups and 64 tertiary amine groups. The positive charge below pH 5 is a result of the protonation of the dendrimers tertiary amine groups with no protonation observed above pH 5.[17,18] The negative charge at pH above 5 is due to the ionisation of the carboxylic functional group.[19]

When the electrophoretic mobility and the hydrodynamic diameter is known, it is then possible to calculate the number of uncompensated charges (N_c) using the Lorenz-Stokes equation

$$N_c = \frac{6\pi\eta R_H}{e}\mu_e \times \frac{1}{1\times 10^{11}}$$

where N_c is the uncompensated charge, η is the viscosity (8.9×10^{-3} g cm^{-1} s^{-1}), R_H is the hydrodynamic radius obtained from DLS (cm), μ_e is the mobility measured by the zeta sizer (μm cm V^{-1} s^{-1}), e = 1.602×10^{-19} C. The results are shown in Fig. 2b. The specific adsorption of counter-ions can be observed at high ionic strengths, I = 0.05 M and above, this is manifest by the shift in IEP from pH 5 to pH 4.6.[16]

The effective degree of ionisation (α), which is a ratio of the average number of uncompensated elementary charges (N_c) as shown above to the nominal number of charges per G5.5 PAMAM (N_m) the value of which is 64 for pH < 5 and 256 for pH > 5

$$\alpha = \frac{N_c}{N_m} \times 100$$

The effective degree of ionisation bears a strong dependence on the ionic strength and the pH of the solution as shown in Fig. 3.

The maximum degree of ionisation for G5.5 PAMAM was found to be approximately 7% for ionic strength I = 0.01 M and pH > 9. The degree of ionisation for low ionic strength I = 0.01 M is just over twice as much compared to low ionic strength I = 0.15 M at the same value of pH. The effective degree of ionisation values are due to the charge compen-

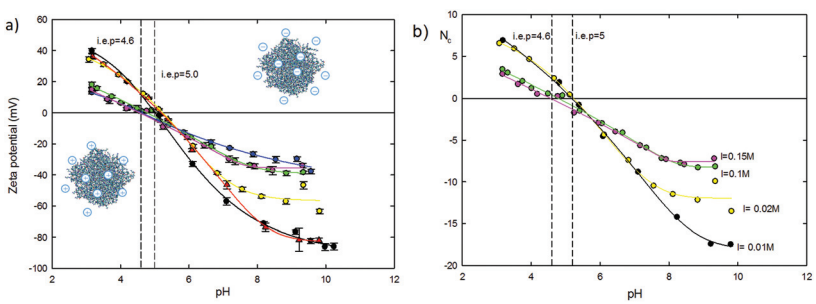


Fig. 2 (a) Dependence of G5.5 PAMAM dendrimer zeta potential (ζ) on pH at varying ionic strength. (b) Dependence of N_c on pH for G5.5 PAMAM dendrimers.

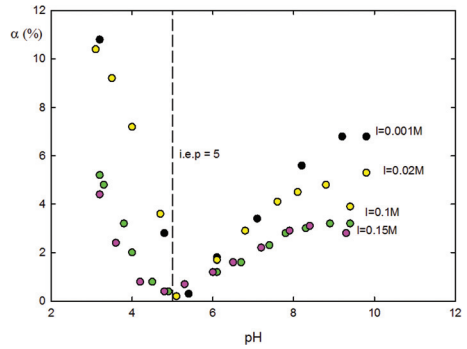


Fig. 3 Dependence of effective degree of ionisation α for G5.5 PAMAM.

sation from counterions condensation on the molecules surface.[20,21]

Using the number of elementary charges per molecule (N_c) and the hydrodynamic radius (R_H), the charge densities (σ) can then be found using the Lorentz-Henry equation

$$\sigma = \frac{N_c}{4\pi {R_H}^2}$$

The values of σ as shown in Table 1 are observed to be negative at high pH and incrementally increase to positive values at low pH, approaching 0 around the IEP. This indicates that as the pH decreases the electric charge of the dendrimer increases, becoming positive above the IEP.[22] From studies performed by Welch it is seen that increasing the surface charge density maximises contact between molecules and the surface of adsorption.[23,24]

The intensity of the absorption band is substantially proportional to the number of chromophore units and can be used to define the morphological structure of dendrimer molecules. Additionally, UV-Vis is a useful method for a better understanding of the properties of the dendrimer, the spectra of which will provide a useful to analyse the complex formation between dendrimer and protein.[25,26] UV-Vis measurements were taken for G5.5 PAMAM c = 500 ppm samples with ionic strengths of I = 0.0001 M, I = 0.01 M and I = 0.15 M NaCl. Fig. 4a shows a comparison of the position of the peaks showing how the wavelength at which the maximums occur differs for changing pH at different ionic strengths.

From the graphs above it can be observed that the wavelength as which the peak occurs increases with increasing pH and for samples with higher ionic strength at the same pH. With suppression of the peaks occurring due to protonation of the dendrimer in high salt concentrations which may cause screening of electrostatic interactions for complex formation.[16,23]

Fig. 4b shows the UV-Vis measurements for G5.5 PAMAM dendrimer of ionic strength 0.01 M measured at pH values ranging from 4 to 10. G5.5 shows a sharp absorption peak at 203 nm. As the pH increases the absorption intensity increase. However, the maximum adsorption wavelength shows little change within the pH range from 3.9 to 9.9. The maximum absorbance peak was observed at pH = 9.9 with wavelength

Table 1 Comparison of uncompensated charge N_c, degree of ionisation α, and charge density σ for G5.5 PAMAM

I = 0.01				I = 0.02				I = 0.05				I = 0.1				I = 0.15			
pH	N_c (e)	α	σ (e nm^{-2})	pH	N_c (e)	α	σ (e nm^{-2})	pH	N_c (e)	α	σ (e nm^{-2})	pH	N_c (e)	α	σ (e nm^{-2})	pH	N_c (e)	α	σ (e nm^{-2})
9.8	−17.5	−6.8	−0.09104	9.8	−13.5	−5.3	−0.07050	9.6	−8.1	−3.2	−0.04198	9.4	−8.2	−3.2	−0.04264	9.3	−7.2	−2.8	−0.03767
9.2	−17.4	−6.8	−0.09072	9.4	−10.0	−3.9	−0.05182	9.2	−6.3	−2.5	−0.03292	8.9	−8.3	−3.2	−0.04326	8.4	−7.9	−3.1	−0.04130
8.2	−14.2	−5.6	−0.04596	8.1	−11.5	−4.5	−0.05993	7.9	−5.7	−2.2	−0.02967	7.8	−7.2	−2.8	−0.03752	7.9	−7.3	−2.9	−0.03814
7.1	−8.8	−3.4	−0.04596	7.6	−10.5	−4.1	−0.05468	7.2	−4.4	−1.7	−0.02827	6.7	−4.1	−1.6	−0.02683	7.2	−5.7	−2.2	−0.03678
6.1	−4.6	−1.8	−0.02378	6.1	−4.4	−1.7	−0.02842	5.9	−2.4	−0.9	−0.01570	6.1	−3.0	−1.2	−0.01961	6.0	−3.0	−1.2	−0.01923
5.4	−0.8	−0.3	−0.00415	5.1	0.4	0.2	0.00278	5.1	−0.9	−0.4	−0.00590	4.9	0.3	0.1	0.00213	5.3	−1.7	−0.7	−0.01132
4.8	1.9	2.9	0.00970	4.7	2.4	3.7	0.01528	4.6	0.2	0.3	0.00120	4.5	0.6	0.9	0.00362	4.2	0.5	0.8	0.00326
3.2	6.9	10.8	0.03591	3.1	6.5	10.2	0.04249	3.2	2.5	3.9	0.01533	3.2	3.4	5.5	0.02231	3.2	2.9	4.5	0.01861

This journal is © The Royal Society of Chemistry 2021

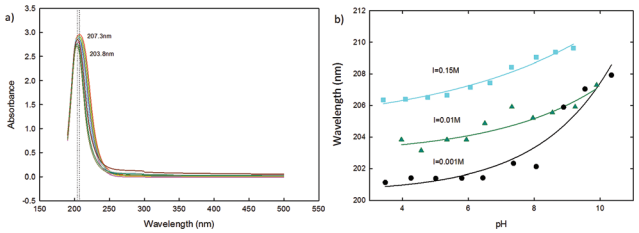


Fig. 4 (a) Wavelength of peak *vs.* pH (b) absorbance spectrum for G5.5 PAMAM c = 500 ppm at I = 0.01 M.

207.3 nm and absorbance 2.96. The minimum absorbance peak was observed at pH = 3.9 with wavelength 203.8 nm and absorbance 2.71. When the pH values increase from 5 to 10 the protonation of periphery functional groups caused more expanded and rigid molecular conformation.

Understanding the physicochemical properties of the dendrimer is essential to any potential application. Table 2 provides a summary of the parameters of the G5.5 PAMAM dendrimer in bulk solution.

Dendrimer–protein complex formation

Several studies have shown that dendrimer-protein complexes have a significant impact on biological processes. The protein coating on the carrier makes it less toxic or invisible to the immune system.[29,30] Moreover, dendrimers influence the interactions between proteins as well as the process of their aggregation, which is especially important in neurodegenerative diseases.[2,31] Many studies indicate that the formation of complexes with BSA or HSA cause a change in the secondary structure of these proteins. From the study of CD measurements, for all types of dendrimers, a decrease in the content of α-helix and an increase in β-sheets and random coil structure are observed.[32,33] The formation of stable complexes with proteins affects not only the secondary structure of the proteins themselves but also the properties of the dendrimers themselves. The screening of some functional groups in the dendrimer molecule should affect the effective charge of the dendriplex. Measurements of electrophoretic mobility allow the tracking of changes taking place during the formation of dendrimer-protein complexes depending on environmental conditions.

Following on from the electrophoretic mobility and zeta potential measurements carried out for G5.5 PAMAM dendrimers the measurements were repeated for mixtures of G5.5 PAMAM and BSA at varying molar ratios to determine what effect complex formation has on the zeta potential and to better understand electrostatic interactions occurring between dendrimer and protein. The zeta potential was calculated from the measured mobility values using Henry's equation with the findings presented in Fig. 5. All samples were mixed at pH 7.5

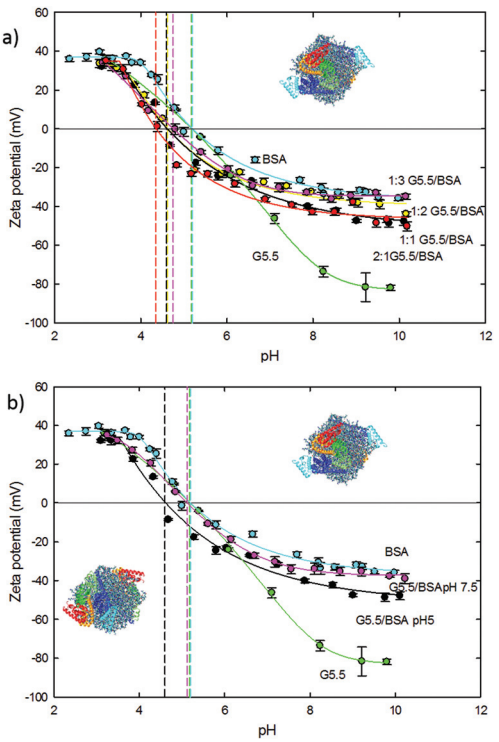


Fig. 5 (a) Dependence of zeta potential on pH for G5.5 PAMAM/BSA complexes with varied molar ratios. (b) Comparison influence of pH of complex formation on zeta potential.

Table 2 Physicochemical properties of G5.5 PAMAM

Characteristic	Value, unit	Remarks
Density, ρ_P	1.2 g cm^{-2}	$\rho = a - be^{(-cn)}$ [21,27]
Molecular weight	52.9 kDa	Manufacturer Dendritech
Diffusion coefficient, D	0.99 ± 0.04 × 10^{-10} m^2 s^{-1}	NMR[21]
Carboxyl surface groups	256	Calculated
Tertiary amine groups	64	Calculated
Total functional groups	320	Calculated
Number of atoms	9156	Calculated[28]
Hydrodynamic radius, R_H	pH > 7.5 R_H = 3.91 nm pH < 7.5 R_H = 3.50 nm	DLS
Hydrodynamic radius, R_H	3.94 ± 0.18 nm	NMR[23]
pK_a carboxyl terminal group	9–10	Potentiometric titration
pK_a tertiary amine group	3–4	Potentiometric titration
i.e. p isoelectric point	5	Electrophoretic mobility
Bare charge N_m from structural formula	−256 e	Calculated
Max effective charge N_c	−17 e	Calculated from electrophoretic mobility

for 30 minutes with their respective molar ratios G5.5 : BSA 2 : 1, 1 : 1, 1 : 2 and 1 : 3.

The IEP for G5.5 PAMAM and BSA are close, pH 5.1 and pH 5.2, respectively. The complexes formed experienced a shift in IEP. At the following ratios of G5.5 : BSA, the IEP were; 2 : 1 had an IEP at pH 4.3, 1 : 1 and 1 : 2 both had IEP at pH 4.6 and 1 : 3 had IEP at pH 4.7.

Another sample of G5.5/BSA was prepared at a 1 : 1 molar ratio again mixing for 30 minutes; however, the pH of the samples was set to 5 before mixing as opposed to pH 7.5 as had been done previously. This permitted to determine whether the pH of mixing had any effect on the complex formed. The effect of counterion condensation of BSA charge that had been observed in the above example was diminished as is shown in Fig. 5b.

Note that zeta potential measurements give the net charge of the molecule. In the case of proteins, where the charge distribution is very heterogeneous, although the net charge of the molecule is negative or positive there are oppositely charged domains on its surface. BSA has 3 main domains, which for example, at pH 7 have two negative domains (domain I −9e, domain II −7.8e) and one positive domain (domain III 1e), respectively.[15]

It should be noted that a change in pH will have an effect on which domain in the BSA structure that will determine dendriplex formation. At pH 5.0, BSA is positive, and dendrimers are positive; under these conditions, the negatively charged I domain will be responsible for the formation of stable complexes with the dendrimers. The situation is different for pH 7.5, in this case, both BSA and the dendrimers have a negative charge. At pH 7.5, domain III that is most positively charged under these conditions will play a role in the formation of the complex. While the trend of changes is very similar, however, at pH 7.5, more significant changes in the value of the zeta potential of the obtained complexes are visible.

In recent years, several models have been developed to which show how dendrimer-protein complexes are formed, including Shcharbin *et al.* 2007- five binding sides,[34] Chiba *et al.* 2010- hot spot model,[35] Shcharbin *et al.* 2007–2015- dendrimer and flexible proteins.[36] For positively charged dendrimers Shcharbin *et al.* identifies five non-specific anionic regions which can be used for binding to albumin. In these centers, aspartic and glutamic acid are located close to each other forming local regions with negative charge. Wang *et al.*,[37] using controlled molecular dynamics, presented a two-stage model in which the process is initially driven by electrostatic forces. Conformational changes arise in the system as a result of electrostatic interactions. The second step involves the dendrimer molecule's inner shells and determines the interaction of the hydrophobic forces. Molecular dynamics clearly show that the dendrimer's outer shell and the dendrimer molecule's internal structure play an essential role in their behavior in the context of protein systems. Molecular dynamics makes it possible to identify key amino acids involved in the formation of the dendrimer-protein complexes and to observe conformational changes in the system and the contribution of hydrophobic forces.[38–40] Experimental methods such as AFM confirm the tendency of the dendrimer molecule to undergo conformational changes. The degree of deformation of the molecule depends on the type, generation and degree of functional groups' protonation under given conditions. For sulphonate-terminated dendrimers, González-García *et al.*[41] proposed the preferential role of the weak dipole–dipole or ion-dipole interactions between the hydrophilic albumin residues and the dendrimer surface.[42] MD simulations of BSA adsorption on the negative surface indicate that it is the positively charged amino acids of domain III that will influence the molecule's final orientation at this surface. Based on these works, it can be concluded that in the case of G5.5 at pH = 7.5, it is principally the positively charged amino acids located in domain III that will determine the formation of a stable complex. The presence of Tryptophan (Trp) residues in BSA is manifest in UV-vis spectra by a peak at 278 nm. From the analysis of the UV-vis spectra of the from the mixtures of G5.5/BSA it is possible to determine whether complex formation has occurred and to determine the ratio of formed complexes. From the qualitative analysis of the UV-vis spectra, there is evidence of the formation of G5.5/BSA complexes of varying ratios from the suppression of Trp peaks at wavelength 278 nm as shown in Fig. 6. The peaks for G5.5 PAMAM were also examined at this wavelength to show there are no competing peaks from tertiary amine protonation for example.

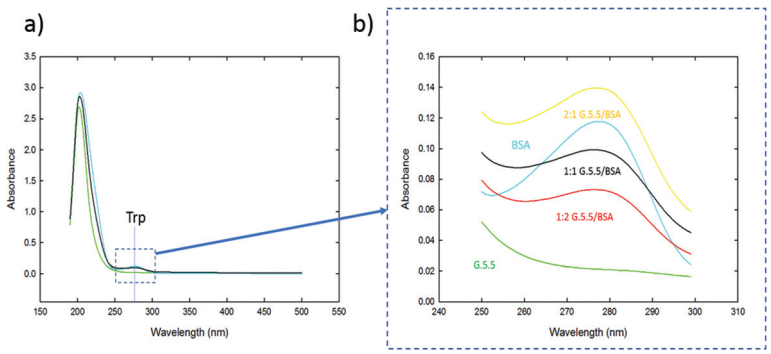


Fig. 6 (a) UV-vis spectra G5.5 + BSA indicating Trp position. (b) Comparison of UV-vis spectra for varying compositions of G5.5/BSA complexes.

This journal is © The Royal Society of Chemistry 2021

Table 3 Comparison of characteristics of G5.5/BSA complexes formed

Ratio G5.5 : BSA	2 : 1	1 : 1	1 : 2	1 : 3
Effective ratio G5.5 : BSA (from UV-vis)	1 : 0.25	1 : 0.47	1 : 0.73	1 : 1.68
Zeta potential (ζ)	−41 mV	−38 mV	−33.4 mV	−32 mV
DLS R_H	Aggregates	4.06 nm	4.15 nm	3.95 nm

By using the relationship between absorbance and concentration in the Beer–Lambert law, it is possible to determine the ratio of G5.5 PAMAM to BSA in the formed complexes. Table 3 shows the effective concentration in the formed complex, assuming that the effective concentration of G5.5 PAMAM in the complex is the same as the initial concentration.

Here it can be seen that the physicochemical properties of the complex such as zeta potential and size are altered depending on the effective ratio in the formed complexes. From the UV-vis measurements, it is shown that the maximum ratio is two BSA molecules per molecule of the dendrimer. In the case of an excess of dendrimer compared to the protein the system is characterized by more negative zeta potential values, while also tending to aggregate. It follows that the excess of dendrimers destabilizes the entire system, and in particular the protein structure, which is confirmed in tests by circular dichroism.

In the dendriplex formation process, not only the charge effect of the dendrimer molecule but also the size effect should be considered.[38] As shown by Chiba *et al.* the highest efficiency is achieved when the size of the protein is comparable to the size of the dendrimer.[35] In the case of G5.5, this parameter seems optimal. The shape of the BSA is comparable to a triangular prism with sides equal 8 nm estimated by XRD or 9.2 nm by AFM and height 3 nm.[43]

If the formation of dendriplexes changes the charge of the molecule, it should be evident in the behavior of the dendriplexes on a surface with a controlled homogeneous surface charge distribution. One of the methods used to monitor the phenomena occurring at the interface is quartz crystal microbalance. This method allows not only the tracking of the adsorption kinetics, determine the adsorbed mass but also estimated the thickness of the layer and the viscoelastic properties of the resulting films.

Modification of surfaces using dendrimers is a valuable alternative provided to modification by self-assembled monolayers of linear polymers.[22,44] In this project, the adsorption of dendrimers was examined as a function of environmental conditions such as concentration and ionic strength. The use of QCM-D and contact angle it was used to determine the effectiveness of adsorption and thickness of films formed by G5.5 PAMAM dendrimers and BSA.

The effect of pH on the effectiveness of adsorption was examined when adsorbing two layers, one of BSA and one of G5.5 PAMAM. The impact of the order in which they are adsorbed was also tested. In each case the first layer (G5.5 or BSA) was adsorbed at pH 4.8 with I = 0.01 M for 45 minutes, then the sensor was rinsed passing NaCl I = 0.01 M at pH 4.8 for 45 minutes, then the second layer (I = 0.01 M) was adsorbed once at pH 4.8 then repeating the experiment at pH 7.5 for 45 minutes, then the surface was again rinsed for all cases at pH 7.5 with NaCl I = 0.01 M for 45 minutes. For all measurements, BSA and G5.5 concentrations were kept constant at 250 ppm. The first layer was adsorbed at pH 4.8 for all experiments, where BSA and G5.5 are positively charged because the gold sensor, which was used as support for adsorption, is negatively charged in this condition.[45] It is not possible to directly adsorb G5.5 dendrimers on the gold surface at pH 7.5, when dendrimers and gold surface are negatively charged.

Using the measurements for mass adsorbed and the molecular weight of BSA and G5.5 it is possible to determine the surface concentration (molecules per cm^2) and the nominal thickness of the layer adsorbed on the surface. Comparing the measurements of mass adsorbed in all four cases, as shown in Fig. 7, it can be seen that the mass of the first layer adsorbed is almost the same. The mass of the second layer is at least twice as low for each case, with more mass adsorbed at pH 4.8 and a comparative increase of mass when G5.5 is second.

The situation of the G5.5 adsorption efficiency on the surface of the protein film is unusual. In the case of pH 4.8, the adsorbed mass is about 300 ng cm^{-2} G5.5, while a change in pH to 7.5 causes a decrease in G5.5 adsorption to the level

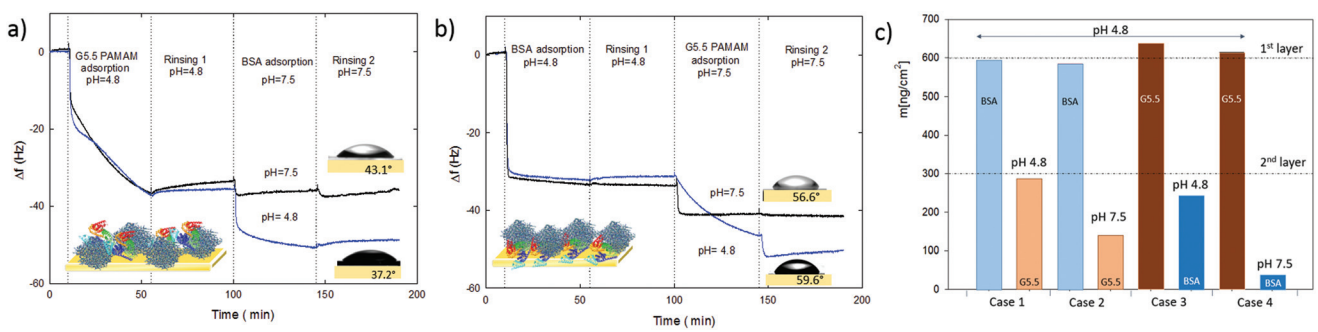


Fig. 7 (a) Dependence of Δf on time for BSA adsorption first, and the contact angle of the sensor measured after adsorption. (b) Dependence of Δf on time for G5.5 PAMAM adsorption first, and the contact angle of the sensor measured after adsorption. (c) Comparison of 4 bilayer adsorption cases, comparing mass of each layer adsorbed.

of 150 ng cm^{-2}. At pH 4.8, it is the tertiary amine groups that will determine the adsorption process, while at pH 7.5, the protonation of the molecule will change, and negative carboxylic groups will determine the adsorption efficiency of dendrimers. At the same time, it should be remembered that BSA adsorbing on the negatively charged surface of domain III, which has the highest positive charge, and thus the negative domains I and II are directed towards the outside of the layer. The more negatively charged domains are less effective in interacting with G.5.5 molecules, which at pH 7.5 are also negatively charged. This shows that by selecting the adsorption conditions, we can effectively control the process of bi-layer formation because electrostatic interactions play a decisive role in this case.

This experiment clearly shows that the interaction of G5.5 dendrimers with proteins will vary depending on environmental conditions. The unique behavior of G 5.5 dendrimers is mainly related to the change in the net charge of the molecule from positive to negative.

The properties of the bilayers were additionally verified by measuring the contact angle of the surface. There is a heterogeneous charge distribution across the surface of the gold sensor with the wettability measured being altered depending on the order of components adsorbed to the sensor. When G5.5 is the last layer, the contact angle is 59.6°–56.6°. When BSA is adsorbed at the end, the contact angle is lower between 37.2°–43.1°. The value of the contact angle in this case is close to the value obtained for the BSA monolayer on different surfaces.[43,46] In both cases the contact angle is smaller and the surface is more hydrophilic when the last adsorbed layer is BSA compared to G5.5 PAMAM being adsorbed last.

The question is whether the complexes formed in the volume of the solution will have the same properties as the bilayer complexes formed on the gold surface? In order to verify this issue, G5.5/BSA complexes were adsorbed on the gold surface using the QCM-D method.

Two complexes were then formed by combining 250 ppm G5.5 PAMAM with 250 ppm BSA at pH 4.8 and pH 7.5 with ionic strength I = 0.01 M. Each of the samples was adsorbed onto a gold surface with QCM-D for 45 minutes and then rinsed with NaCl (I = 0.01 M) with the same pH corresponding to the complex for 45 minutes.

Comparing the adsorption of the complex to the adsorption of G5.5/BSA bilayers it can be seen that the amount adsorbed for complexes in the same pH compared to bilayers is smaller as shown in Fig. 8.

Considering the zeta potential of the complexes, its value is more negative compared to both the BSA molecule and the dendrimers at pH 4.8. At pH 7.5, the zeta value of the potential is also more negative than for BSA, but close to that of the dendrimers. If the complexes are adsorbed on the negatively charged gold surface, the adsorption efficiency will be much lower for the more negatively charged complex. As in the case of adsorption of bi-layers, electrostatic interactions will determine the behaviour of the complexes on the adsorption surface, which confirms the much lower adsorption efficiency of the complexes at pH 7.5 compared to pH 4.8.

It is known that the interaction of proteins with various types of surfaces causes a change in the secondary structure of the protein.[32,33] A method that is useful for assessing changes in protein structure is circular dichroism. Circular dichroism measurements were taken to determine the effects of complex formation on the structure of BSA. Two sets of measurements were taken one with high concentrations of G5.5 PAMAM and one with low concentration for pH 4.8 and 7.5. All samples were prepared with NaCl I = 0.01 M. For low concentrations, the concentration of dendrimers was assumed at the level of 12.5 ppm to 50 ppm. For high concentrations ranging from 500 ppm to 1500 ppm.

Analysis of the CD measurements gives insight into the structural stability of BSA. From the CD spectra for high G5.5 concentration (Fig. 9a) a large decrease in α-helix is observed manifest by the peak at 195 nm for BSA disappearing for BSA + G5.5 as well as the shift of the 208 nm peak. There is also an increase in β-sheets and random coil.

From the CD spectra for the G5.5/BSA samples with low G5.5 PAMAM concentration (Fig. 9b) a decrease in α-helix is again observed by some decrease in the peak at 195 nm. There is again an increase in β-sheets and random coil.

From the CD measurement results it was concluded that the dendrimer had a strong effect in decreasing the α-helix

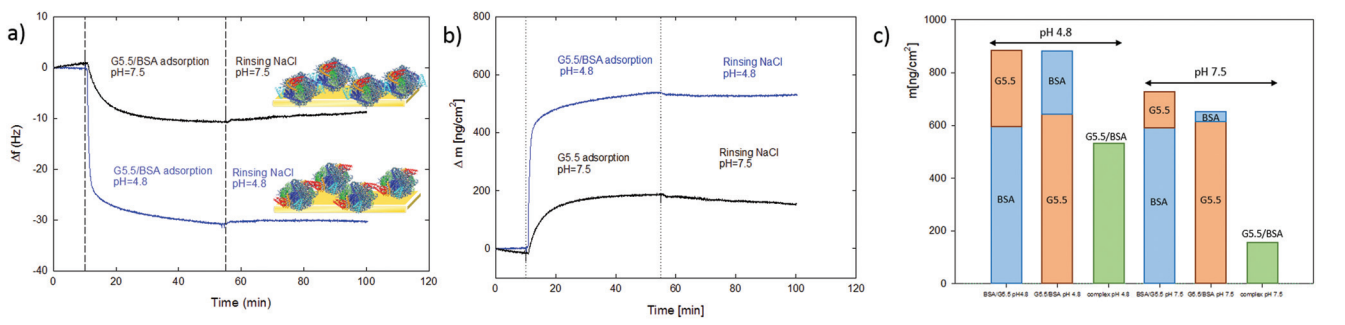


Fig. 8 (a) Dependence of Δf on time for G5.5/BSA complexes in pH 4.8 and pH 7.5. (b) Dependence of mass adsorbed on time for G5.5/BSA complexes in pH 4.8 and pH 7.5. (c) Comparison of mass adsorbed for formation of bilayer on the surface and adsorption of complex from bulk.

This journal is © The Royal Society of Chemistry 2021

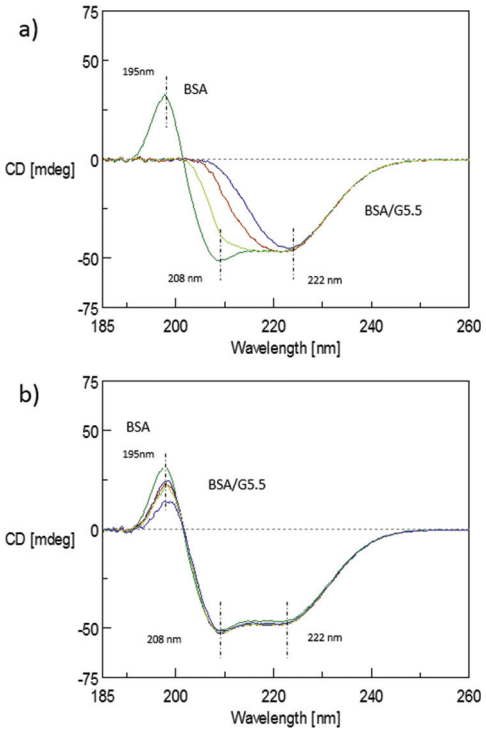


Fig. 9 (a) CD measurements for high concentration G5.5 PAMAM in G5.5/BSA complex. (b) CD measurements for low concentration G5.5 PAMAM in G5.5/BSA complex.

structure. The presence of dendrimer lead to changes in the structure of proteins. Experimental results showed that G5.5 PAMAM interacts strongly with BSA. Strong interactions caused by electrostatic interactions between dendrimer and BSA molecules and the reorganisation of BSA domains. The results obtained were consistent with those found in literature, where dendrimer binding was noted to alter BSA conformation with major reductions in α-helix and increased random coil and turn structures, indicating partial protein unfolding.[33] With similar results noted for interactions occurring between G4 PAMAM and human serum albumin.[32]

Conclusions

The physicochemical properties of a nanocarrier are essential parameters in drug delivery system design (DDS). Measurements of the electrophoretic mobility showed that the dendrimer's charge in the range of pH 3–5 is positive due to the protonation of the tertiary amine groups. Above pH 5, the dendrimer was found to have a negative charge induced by surface carboxyl groups. The isoelectric point for G5.5 occurs at pH 5. DLS measurements showed a significant change in the hydrodynamic radius of the dendrimer molecule. The particle size in the low pH range is equal 3.5 nm, but above pH 7.5 it increases as a result of protonation of the carboxyl group.

The formation of a stable dendrimer-protein complex was monitored using the UV-vis method and the zeta potential measurements. The presence in the UV-Vis spectrum of the peak at 278 nm, which comes from tryptophan in the BSA molecule, confirms the immobilization of protein molecules on the dendrimer surface. Moreover, the decrease in surface potential also confirms that protein molecules bind to the dendrimer's surface. The properties and stability of the resulting complexes were additionally monitored using the QCM-D method. The complexes were noted to irreversibly adsorb on the gold surface. This is different to the dendrimer itself, which tends to desorb at high pH when negatively charged. No significant differences in the arrangement are observed when creating a bilayer. Only the wettability of the surface varies with the outer adsorption layer. The contact angle is lower when the BSA layer is the last layer to be adsorbed on the sensor. CD measurements show that BSA's secondary structure is altered by interaction with G5.5 dendrimers, the most significant changes being seen with a large excess of dendrimers to protein.

It was concluded that BSA bound to the surface of G5.5 PAMAM surface through the positively charged domain III, forming a protein shell or corona on the surface of the dendrimer carriers.[47] This proved to be concurrent with studies of nanoparticle DDS and protein interactions. This benefits its potential use in DDS as it inhibits the adsorption of plasma proteins to the dendrimer surface, reduces the toxicity of the dendrimer, and prevents rapid clearance from the blood, increasing circulation time. The biological properties and bioavailability are also improved when the stable protein-dendrimer complex is formed.[47–49]

Conflicts of interest

There are no conflicts to declare.

Acknowledgements

This work was partially supported by project NCN OPUS 2016/23/B/02788, ERASMUS + UK GLASGOW 02.

Notes and references

1 M. R. C. Marques, Q. Choo, M. Ashtikar, T. C. Rocha, S. Bremer-Hoffmann and M. G. Wacker, Nanomedicines - Tiny particles and big challenges, *Adv. Drug Delivery Rev.*, 2019, **151–152**, 23–43, DOI: 10.1016/j.addr.2019.06.003.

2 B. Klajnert, M. Cortijo-Arellano, J. Cladera and M. Bryszewska, Influence of dendrimer's structure on its activity against amyloid fibril formation, *Biochem. Biophys. Res. Commun.*, 2006, **345**(1), 21–28, DOI: 10.1016/j.bbrc.2006.04.041.

3 L. Vroman and A. L. Adams, Identification of rapid changes at plasma-solid interfaces, *J. Biomed. Mater. Res.*, 1969, **3**(1), 43–67, DOI: 10.1002/jbm.820030106.

4 L. Vroman, A. L. Adams and M. Klings, Interactions among human blood proteins at interfaces, *Fed. Proc.*, 1971, **30**(5), 1494–1502.

5 A. E. Nel, L. Mädler, D. Velegol, *et al.*, Understanding biophysicochemical interactions at the nano–bio interface, *Nat. Mater.*, 2009, **8**(7), 543–557, DOI: 10.1038/nmat2442.

6 P. Kesharwani, K. Jain and N. K. Jain, Dendrimer as nanocarrier for drug delivery, *Prog. Polym. Sci.*, 2014, **39**(2), 268–307, DOI: 10.1016/j.progpolymsci.2013.07.005.

7 A. Åkesson, M. Cárdenas, G. Elia, M. P. Monopoli and K. A. Dawson, The protein corona of dendrimers: PAMAM binds and activates complement proteins in human plasma in a generation dependent manner, *RSC Adv.*, 2012, **2**(30), 11245–11248, DOI: 10.1039/C2RA21866F.

8 F. Ruggeri, A. Åkesson, P.-Y. Chapuis, *et al.*, The dendrimer impact on vesicles can be tuned based on the lipid bilayer charge and the presence of albumin, *Soft Matter*, 2013, **9**(37), 8862–8870, DOI: 10.1039/C3SM50603G.

9 M. Lundqvist, J. Stigler, G. Elia, I. Lynch, T. Cedervall and K. A. Dawson, Nanoparticle size and surface properties determine the protein corona with possible implications for biological impacts, *Proc. Natl. Acad. Sci. U. S. A.*, 2008, **105**(38), 14265–14270, DOI: 10.1073/pnas.0805135105.

10 G. Sahay, D. Y. Alakhova and A. V. Kabanov, Endocytosis of nanomedicines, *J. Controlled Release*, 2010, **145**(3), 182–195, DOI: 10.1016/j.jconrel.2010.01.036.

11 N. Boon, G. I. Guerrero-García, R. Van Roij and M. O. De La Cruz, Effective charges and virial pressure of concentrated macroion solutions, *Proc. Natl. Acad. Sci. U. S. A.*, 2015, **112**(30), 9242–9246, DOI: 10.1073/pnas.1511798112.

12 P. R. Majhi, R. R. Ganta, R. P. Vanam, E. Seyrek, K. Giger and P. L. Dubin, Electrostatically driven protein aggregation: β-Lctoglobulin at low ionic strength, *Langmuir*, 2006, **22**(22), 9150–9159, DOI: 10.1021/la053528w.

13 B. Fritzinger and U. Scheler, Scaling behaviour of PAMAM dendrimers determined by diffusion NMR, *Macromol. Chem. Phys.*, 2005, **206**(13), 1288–1291, DOI: 10.1002/macp.200500048.

14 M. A. Van Dongen, B. G. Orr and M. M. Banaszak Holl, Diffusion NMR study of generation-five PAMAM dendrimer materials, *J. Phys. Chem. B*, 2014, **118**(25), 7195–7202, DOI: 10.1021/jp504059p.

15 K. Kubiak-Ossowska, K. Tokarczyk, B. Jachimska and P. A. Mulheran, Bovine Serum Albumin Adsorption at a Silica Surface Explored by Simulation and Experiment, *J. Phys. Chem. B*, 2017, **121**(16), 3975–3986, DOI: 10.1021/acs.jpcb.7b01637.

16 K. Tokarczyk and B. Jachimska, Quantitative interpretation of PAMAM dendrimers adsorption on silica surface, *J. Colloid Interface Sci.*, 2017, **503**, 86–94, DOI: 10.1016/j.jcis.2017.05.002.

17 D. A. Tomalia, Birth of a new macromolecular architecture: Dendrimers as quantized building blocks for nanoscale synthetic polymer chemistry, *Prog. Polym. Sci.*, 2005, **30**(3–4), 294–324, DOI: 10.1016/j.progpolymsci.2005.01.007.

18 D. A. Tomalia, H. Baker, J. Dewald, *et al.*, A new class of polymers: Starburst-dendritic macromolecules, *Polym. J.*, 2002, **34**(5 2), 132–147.

19 G. J. M. Koper and M. Borkovec, Proton binding by linear, branched, and hyperbranched polyelectrolytes, *Polymer*, 2010, **51**(24), 5649–5662, DOI: 10.1016/j.polymer.2010.08.067.

20 S. Swiatek, P. Komorek and B. Jachimska, Adsorption of β-lactoglobulin A on gold surface determined in situ by QCM-D measurements, *Food Hydrocolloids*, 2019, **91**(August 2018), 48–56, DOI: 10.1016/j.foodhyd.2019.01.007.

21 P. K. Maiti and R. Messina, Counterion distribution and ζ-potential in PAMAM dendrimer, *Macromolecules*, 2008, **41**(13), 5002–5006, DOI: 10.1021/ma7025435.

22 K. Tokarczyk and B. Jachimska, Characterization of G4 PAMAM dendrimer complexes with 5-fluorouracil and their interactions with bovine serum albumin, *Colloids Surf., A*, 2019, **561**(October 2018), 357–363, DOI: 10.1016/j.colsurfa.2018.10.080.

23 B. Jachimska and K. Tokarczyk, Combining Surface Plasmon Resonance and Quartz Crystal Microbalance to Determine Hydration of Dendrimer Monolayers, *J. Phys. Chem. C*, 2016, **120**(35), 19678–19685, DOI: 10.1021/acs.jpcc.6b05020.

24 B. Jachimska, *Physicochemical Characterization of PAMAM Dendrimer as a Multifunctional Nanocarriers*. Elsevier Inc., 2019. DOI: 10.1016/b978-0-12-816504-1.00003-x.

25 B. Devarakonda, D. P. Otto, A. Judefeind, R. A. Hill and M. M. de Villiers, Effect of pH on the solubility and release of furosemide from polyamidoamine (PAMAM) dendrimer complexes, *Int. J. Pharm.*, 2007, **345**(1–2), 142–153, DOI: 10.1016/j.ijpharm.2007.05.039.

26 Y. Wang, S. Niu, Z. Zhang, Y. Xie, C. Yuan, H. Wang, D. Fu, *et al.*, Reversible pH manipulation of the fluorescence emission from sectorial poly(amido amine) dendrimers, *J. Nanosci. Nanotechnol.*, 2010, **10**(7), 4227–4233, DOI: 10.1166/jnn.2010.2195.

27 R. Dzakpasu and D. Axelrod, Dynamic light scattering microscopy. A novel optical technique to image submicroscopic motions. I: Theory, *Biophys. J.*, 2004, **87**(2), 1279–1287, DOI: 10.1529/biophysj.103.033837.

28 B. Jachimska, M. Łapczyńska and S. Zapotoczny, Reversible swelling process of sixth-generation poly(amido amine) dendrimers molecule as determined by quartz crystal microbalance technique, *J. Phys. Chem. C*, 2013, **117**(2), 1136–1145, DOI: 10.1021/jp307832p.

29 I. Lynch, T. Cedervall, M. Lundqvist, C. Cabaleiro-Lago, S. Linse and K. A. Dawson, The nanoparticle-protein complex as a biological entity; a complex fluids and surface science challenge for the 21st century, *Adv. Colloid Interface Sci.*, 2007, **134–135**, 167–174, DOI: 10.1016/j.cis.2007.04.021.

30 I. Lynch, A. Salvati and K. A. Dawson, Protein-nanoparticle interactions: What does the cell see?, *Nat. Nanotechnol.*, 2009, **4**(9), 546–547, DOI: 10.1038/nnano.2009.248.

 This journal is © The Royal Society of Chemistry 2021

31 M. Bryszewska and B. Klajnert, Dendrimers in biomedical applications, *Curr. Med. Chem.*, 2012, **19**(29), 4895, DOI: 10.2174/0929867311209024895.

32 S. Sekowski, A. Buczkowski, B. Palecz and T. Gabryelak, Interaction of polyamidoamine (PAMAM) succinamic acid dendrimers generation 4 with human serum albumin, *Spectrochim. Acta, Part A*, 2011, **81**(1), 706–710, DOI: 10.1016/j.saa.2011.07.009.

33 J. S. Mandeville and H. A. Tajmir-Riahi, Complexes of dendrimers with bovine serum albumin, *Biomacromolecules*, 2010, **11**(2), 465–472, DOI: 10.1021/bm9011979.

34 D. Shcharbin, M. Janicka, M. Wasiak, B. Palecz, M. Przybyszewska, M. Zaborski and M. Bryszewska, Serum Albumins Have Five Sites for Binding of Cationic Dendrimers, *Biochim. Biophys. Acta, Proteins Proteomics*, 2007, **1774**(7), 946–951, DOI: 10.1016/j.bbapap.2007.04.016.

35 F. Chiba, T. Chou, L. J. Twyman and M. Wagstaff, Dendrimers as size selective inhibitors to protein–protein binding, *Chem. Commun.*, 2008, (36), 4351–4353, DOI: 10.1039/B806517A.

36 D. Shcharbina, N. Shcharbina, V. Dzmitruk, E. Pedziwiatr-Werbicka, M. Ionov, S. Mignani, F. J. de la Mata, R. Gómez, M. A. Munoz-Fernánd, J.-P. Majoral and M. Bryszewska, Dendrimer-protein interactions versus dendrimer-based nanomedicine, *Colloids Surf., B*, 2017, **152**, 414–422, DOI: 10.1016/j.colsurfb.2017.01.041.

37 B. Wang, Y. Sun, T. P. Davis, P. C. Ke, Y. Wu and F. Ding, Understanding Effects of PAMAM Dendrimer Size and Surface Chemistry on Serum Protein Binding with Discrete Molecular Dynamics Simulations, *ACS Sustainable Chem. Eng.*, 2018, **6**, 11704–11715, DOI: 10.1021/acssuschemeng.8b01959.

38 J. Giri, M. S. Diallo, A. J. Simpson, *et al.*, Interactions of poly(amidoamine) dendrimers with human serum albumin: binding constants and mechanisms, *ACS Nano*, 2011, **5**(5), 3456–3468, DOI: 10.1021/nn1021007.

39 B. Nandy, D. H. Bindu, N. M. Dixit and P. K. Maiti, Simulations reveal that the HIV-1 gp120-CD4 complex dissociates via complex pathways and is a potential target of the polyamidoamine (PAMAM) dendrimer, *J. Chem. Phys.*, 2013, **139**, 024905, DOI: 10.1063/1.4812801.

40 B. Nandy, S. Saurabh, A. K. Sahoo, N. M. Dixit and P. K. Maiti, The SPL7013 dendrimer destabilizes the HIV-1 gp120–CD4 complex, *Nanoscale*, 2015, **7**(44), 18628–18641, DOI: 10.1039/c5nr04632g.

41 E. González-García, M. Maly, F. J. de la Mata, R. Gómez, M. L. Marina and M. C. García, Factors affecting interactions between sulphonate-terminated dendrimers and proteins: A three case study, *Colloids Surf., B*, 2017, **149**, 196–205, DOI: 10.1016/j.colsurfb.2016.10.020.

42 K. Kubiak-Ossowska, B. Jachimska and P. Mulheran, How Negatively Charged Proteins Adsorb to Negatively Charged Surfaces a Molecular Dynamics Study of BSA Adsorption on Silica, *J. Phys. Chem. B*, 2016, **120**(40), 10463–10468, DOI: 10.1021/acs.jpcb.6b07646.

43 B. Jachimska, K. Tokarczyk, M. Łapczyńska, A. Puciul-Malinowska and S. Zapotoczny, Structure of bovine serum albumin adsorbed on silica investigated by quartz crystal microbalance, *Colloids Surf., A*, 2016, **489**, 163–172, DOI: 10.1016/j.colsurfa.2015.10.033.

44 M. Zhang, J. Wang and P. Zhang, Controllable Self-Assembly of Amphiphilic Dendrimers on a Silica Surface: The Effect of Molecular Topological Structure and Salinity, *J. Phys. Chem. B*, 2016, **120**(42), 10990–10999, DOI: 10.1021/acs.jpcb.6b05673.

45 B. Jachimska, S. Świątek, J. I. Loch, K. Lewiński and T. Luxbacher, Adsorption effectiveness of β-lactoglobulin onto gold surface determined by quartz crystal microbalance, *Bioelectrochemistry*, 2018, **121**(January), 95–104, DOI: 10.1016/j.bioelechem.2018.01.010.

46 B. Jachimska and A. Pajor, Physico-chemical characterization of bovine serum albumin in solution and as deposited on surfaces, *Bioelectrochemistry*, 2012, **87**, 138–146, DOI: 10.1016/j.bioelechem.2011.09.004.

47 Q. Peng, S. Zhang, Q. Yang, *et al.*, Preformed albumin corona, a protective coating for nanoparticles based drug delivery system, *Biomaterials*, 2013, **34**(33), 8521–8530, DOI: 10.1016/j.biomaterials.2013.07.102.

48 D. Pozzi, G. Caracciolo, A. L. Capriotti, *et al.*, Surface chemistry and serum type both determine the nanoparticle-protein corona, *J. Proteomics*, 2015, **119**, 209–217, DOI: 10.1016/j.jprot.2015.02.009.

49 M. Aoyama, K. Hata, K. Higashisaka, K. Nagano, Y. Yoshioka and Y. Tsutsumi, Clusterin in the protein corona plays a key role in the stealth effect of nanoparticles against phagocytes, *Biochem. Biophys. Res. Commun.*, 2016, **480**(4), 690–695, DOI: 10.1016/j.bbrc.2016.10.121.